

## Plasma Synthesis of Rare Earth Doped Integrated Optical Waveguides\*

S. Raoux<sup>@</sup>, S. Anders, K.M. Yu, I.C. Ivanov<sup>\*\*</sup>, and I.G. Brown

Lawrence Berkeley Laboratory  
University of California  
Berkeley, CA 94720

March 1995

\* This work was supported in part by the U.S. Department of Energy, Office of Basic Energy Sciences, Division of Advanced Energy Projects, under Contract No. DE-AC03-76SF00098.

@ On leave from DGA/DRET, 4 Rue de la porte-d'Issy, F75015 PARIS.

\*\* Charles Evans & Associates, 301 Chesapeake Drive, Redwood City, CA 94063.

## **DISCLAIMER**

This report was prepared as an account of work sponsored by an agency of the United States Government. Neither the United States Government nor any agency thereof, nor any of their employees, make any warranty, express or implied, or assumes any legal liability or responsibility for the accuracy, completeness, or usefulness of any information, apparatus, product, or process disclosed, or represents that its use would not infringe privately owned rights. Reference herein to any specific commercial product, process, or service by trade name, trademark, manufacturer, or otherwise does not necessarily constitute or imply its endorsement, recommendation, or favoring by the United States Government or any agency thereof. The views and opinions of authors expressed herein do not necessarily state or reflect those of the United States Government or any agency thereof.

## **DISCLAIMER**

**Portions of this document may be illegible in electronic image products. Images are produced from the best available original document.**

## PLASMA SYNTHESIS OF RARE EARTH DOPED INTEGRATED OPTICAL WAVEGUIDES

S. Raoux<sup>@\*</sup>, S. Anders\*, K. M. Yu\*, I. C. Ivanov<sup>°</sup>, and I. G. Brown\*.

\*Lawrence Berkeley Laboratory, MS 53, Berkeley CA 94720

<sup>°</sup>Charles Evans & Associates, 301 Chesapeake Drive, Redwood City, CA 94063.

<sup>@</sup>On leave from DGA/DRET, 4 Rue de la porte-d'Issy, F75015 PARIS.

### ABSTRACT

We describe a novel means for the production of optically active planar waveguides. The technique makes use of a low energy plasma deposition. Cathodic-arc-produced metal plasmas are used for the metallic components of the films and gases are added to form compound films. Here we discuss the synthesis of  $\text{Al}_{2-x}\text{Er}_x\text{O}_3$  thin films. The erbium concentration (x) can vary from 0 to 100% and the thickness of the film can be from Angstroms to microns. In such material, at high active center concentration (x=1% to 20%), erbium ions give rise to room temperature  $1.53\mu\text{m}$  emission which has minimum loss in silica-based optical fibers. With this technique, multilayer integrated planar waveguide structures can be grown, such as  $\text{Al}_2\text{O}_3/\text{Al}_{2-x}\text{Er}_x\text{O}_3/\text{Al}_2\text{O}_3/\text{Si}$ , for example.

### INTRODUCTION

The monolithic integration of electronic and photonic devices onto a single chip has become the focus of considerable research effort worldwide in recent years<sup>1</sup>. Advances in these optoelectronic integrated circuits, or OEICs, are driven by the needs of second-generation photonic systems including optical interconnects, optical computing, signal processing and communications. This new technology has the potential to boost considerably the sophistication and performance of existing and proposed advanced photonic systems. Future components will be capable of sending information at data rates greater than 1 Gb/sec, with highly parallel architecture and low power consumption<sup>2</sup>.

Key research and development concerns include both materials design and processing issues. Optoelectronic integrated circuits combine devices that implement optical functions in a guided wave structure with electronic semiconductor devices formed on the same substrate. The electronics of such components is now well mastered, and the next challenge is the development of the optical functions, which are based either on semiconductor materials (SC quantum wells) or on dielectric waveguide structures. Our interest is in the latter.

Dielectric waveguide structures are based on multilayer thin film technology. A sandwich is formed in which the central guiding film is of higher refractive index than the surrounding material. Planar waveguides guide light in the vertical direction but provide no lateral confinement. For compatibility with optical fibers and for efficient modulation, strip waveguides are essential and have been fabricated by sputtering, epitaxial layers, ion implantation, ion exchange, and diffusion techniques combined with standard lithographic technology<sup>3-9</sup>. Typical thickness of the films is  $1\mu\text{m}$ . The required geometry of the waveguide depends essentially on the guided wavelength and the difference of refractive indices in the guiding region and the cladding layer material<sup>10,11</sup>. Such optical waveguides are the basic structures leading to advanced OptoElectronic Integrated Circuits or OEICs.

By doping the guiding region with optically active impurities, integrated optical amplifiers and lasers can be fabricated. The principle is the same as for optical fiber amplifiers and lasers. However, multilayer-thin-film technologies allow the formation of waveguides with higher refractive index differences between the guiding region and the surrounding, and the optimum concentration of active optical centers can also be two orders of magnitude greater when incorporated in dielectric waveguide materials<sup>12</sup>. Consequently the typical size of an

integrated amplifier/laser device is about 1 cm, instead of 1m as is typical for optical fiber lasers. By using spiral-strip waveguides it could be possible to make high performance integrated devices.

An important application for such active OEICs is the fabrication of 1.53  $\mu\text{m}$  lasers by doping the waveguide with  $\text{Er}^{3+}$  ions. Importantly, note that the  $^4I_{13/2}$ - $^4I_{15/2}$ ,  $4f^{11}$ -transition of erbium occurs at  $\lambda = 1.53 \mu\text{m}$ , coinciding with the low-loss window for silica-based optical fibers<sup>13</sup>.

In this paper we describe a new tool for the synthesis of  $\text{Al}_2\text{O}_3$  and  $\text{Al}_{2-x}\text{Er}_x\text{O}_3$  thin films on silicon substrates. This synthesis technique can lead to the formation of multilayer structures like  $\text{Al}_2\text{O}_3/\text{Al}_{2-x}\text{Er}_x\text{O}_3/\text{Al}_2\text{O}_3/\text{Si}$  in order to form waveguide structures. We report on the fabrication conditions and the preliminary optical properties of the films.

## CONCEPT AND TECHNOLOGY DESCRIPTION

We have developed some novel plasma techniques for materials modification and the synthesis of advanced materials. These methods include high current metal ion implantation, metal film deposition, plasma synthesis of composite and multilayer films, and the atomic bonding (ion stitching) of these films to the underlying substrate.<sup>14-17</sup>

The plasma tools employed are based on the application of pulsed cathodic arc discharges for the production of intense, directed plumes of highly ionized metal plasma and their utilization for plasma deposition and the generation of ion beams. We refer to this general approach by the acronym MePIIID, for Metal Plasma Immersion Ion Implantation and Deposition. The method combines plasma deposition and ion bombardment techniques to create a powerful and adaptable new technology that is environmentally friendly, highly efficient, can be scaled up to large size, and can synthesize films of a range of materials, including optoelectronic materials.

Figure 1 shows the general experimental configuration for the production of  $\text{Al}_2\text{O}_3$  or  $\text{Al}_{2-x}\text{Er}_x\text{O}_3$  thin films. Two plasma guns can be used (Al and Er). The plasma sources are repetitively pulsed, so that the composition of the film can be tailored by adjusting the pulse duration or amplitude of each plasma gun. Another configuration consist in using a single plasma gun with an Al/Er metal alloy, thereby allowing the formation of fixed-concentration films. Both of these techniques have been tested, the second one leading to very homogeneous thin films with respect to the erbium concentration as a function of depth in the film. The plasma beams are filtered through a curved magnetic duct which directs the beam to the substrate. The formation of oxide material is done by operating in a residual pressure of oxygen. By applying a negative pulsed bias voltage to the substrate, one can combine the film deposition process with a plasma immersion ion bombardment process, so that the film structure can be controlled.

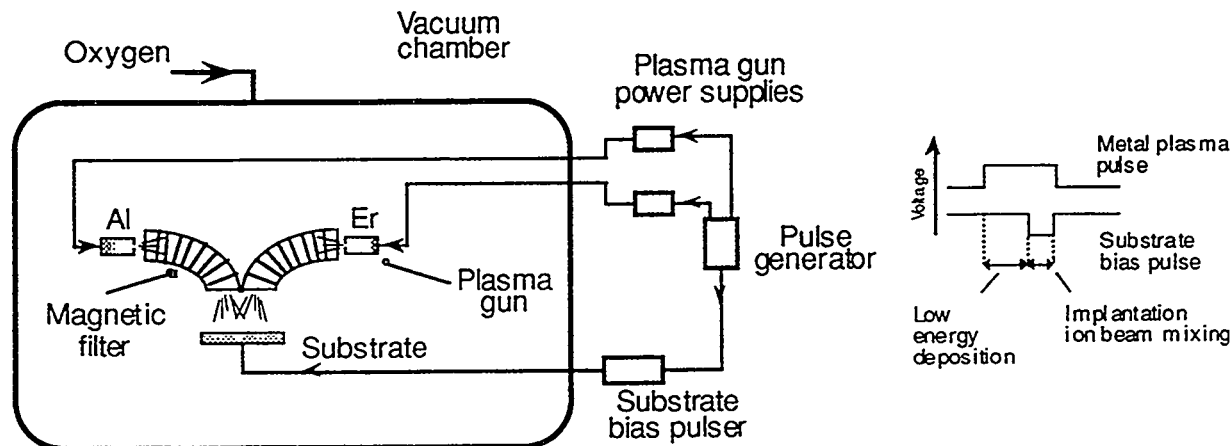


Figure 1 - Schematic of generalized experimental configuration

## Metal plasma production

In the method described here, we use a pulsed miniature cathodic arc plasma gun with an aluminum or an erbium cathode or an Al/Er metal alloy cathode of 0.64 mm diameter. Bigger water-cooled guns (5cm diameter), DC operated, can be used for the production of large scale samples and for industrial applications. A photograph of a miniature plasma gun is shown in figure 2. When the arc discharge takes place between the two electrodes, the plasma necessary for the current transport is formed at spots on the cathode surface. The current density in the cathode spots is very high ( $J \approx 10^{12} \text{A.m}^{-2}$ ) as well as the plasma density which can reach  $n \approx 10^{26} \text{ions.m}^{-3}$ <sup>18</sup>. The cathode material undergoes a transition from its solid phase to the plasma phase via liquid and dense non equilibrium plasma phases. The pressure in the cathode spot is very high ( $P \approx 10^{10} \text{Pa}$ ) and the plasma rapidly expands into the chamber under the intense pressure gradient. In contrast to most gaseous plasmas, the cathodic arc plasma is nearly fully ionized. Each cathode material has its own specific ion charge state distribution (CSD). Table 1 shows the plasma CSD obtained by time-of-flight measurements for plasmas formed from an aluminum, an erbium and an Al/Er alloy cathode (5% Er at. fraction). As can be seen, the ratio Al/Er in the plasma (3.9% Er.at.fraction) is lightly lower than the cathode composition. However, the Er content in the film has been found to be the same as in the plasma.



**Figure 2** Photograph of a version of miniature cathodic arc plasma gun. Observe the cathode material in the interior of the anode.

	Al <sup>+</sup>	Al <sup>2+</sup>	Al <sup>3+</sup>	Total Al	Er <sup>+</sup>	Er <sup>2+</sup>	Er <sup>3+</sup>	Total Er
Aluminum cathode	38	51	11	100	-	-	-	-
Erbium cathode	-	-	-	-	1	63	36	100
Al/Er(5%) cathode	32	56	8.1	96.1	-	2.1	1.8	3.9

**Table 1** Charge state distribution of the plasma for an aluminum, an erbium and an Al/Er alloy cathodes

## Cathodic arc plasmas filtering

Due to the transition of the cathode material from its solid phase to a plasma via a liquid phase and the considerable pressures involved in the process, not only plasma is formed at the cathode surface, but also small liquid droplets and macroparticles. A direct exposure of the substrate to the gun leads to the obtention of highly rough and defective thin films.

A conventional method<sup>18</sup> for separating plasma and macroparticles is to use a curved magnetic field induced by a coil electrically connected in series with the arc current<sup>19,20</sup>. Thus, by directing the plasma beam to a direction 90° off the gun orientation, the plasma is separated from the macroparticles that move in nearly straight lines due to their inertia. The pulsed operation of the plasma gun and the series field coil solves the problem of heat load and permits a high current (typically 300A) for the production of the magnetic field, without any additional power supply. The typical maximum magnetic field in the filter for an arc current of 300A is 80mT.

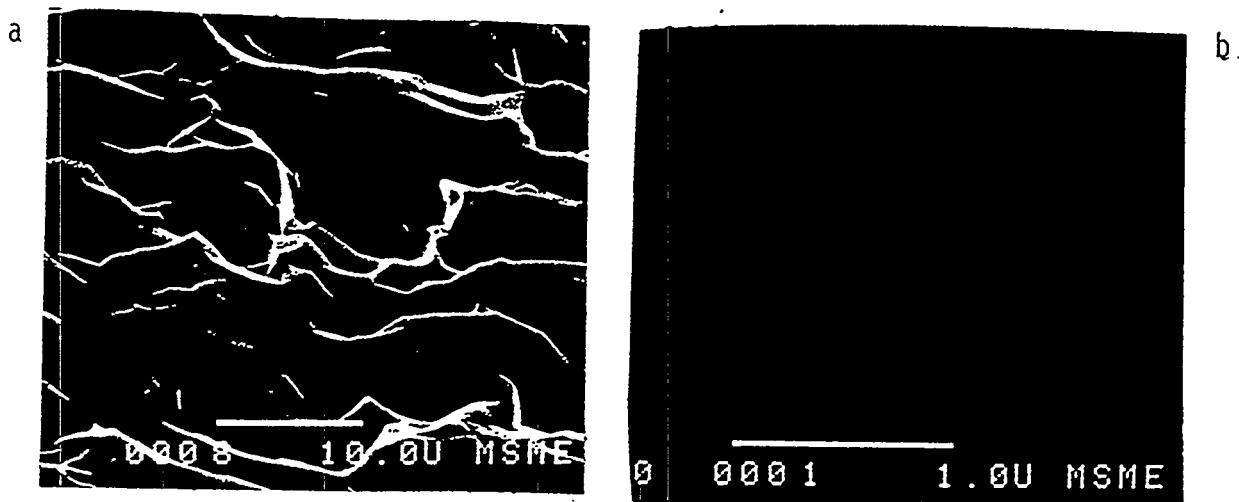


Figure 3 SEM micrographs of an  $\text{Al}_2\text{O}_3$  thin film ( $2000\text{\AA}$ ) deposited on silicon.  
 (a) without magnetic filter.  
 (b) with magnetic filter for the formation of high purity and smooth thin films

Figure 3 shows SEM pictures of  $\text{Al}_2\text{O}_3$  thin films without (a) and with (b) the use of the magnetic filter. It is clear that the use of the magnetic filter leads to the formation of macroparticle free, very smooth and defect-free thin films, on the micrometer scale.

## FORMATION OF THE SAMPLES

The  $\text{Al}_2\text{O}_3$  samples were formed in a residual pressure of oxygen varying from  $1 \times 10^{-5}$  Torr to 20 mTorr. The plasma guns were operated under the following conditions: arc current ( $I_{\text{arc}}=300\text{A}$ ), pulse duration ( $t_{\text{arc}}=5\text{ms}$ ), repetition rate ( $f_{\text{arc}}=2 \text{ pulses}\cdot\text{s}^{-1}$ ). The substrates were maintained at a temperature of  $250^\circ\text{C}$  and negatively biased at ( $V_{\text{bias}}=600\text{V}$ ). The bias is applied for  $2\mu\text{s}$ , every  $8\mu\text{s}$  during the arc pulse duration, so that the low-energy deposition of the incoming ions is alternatively combined with their implantation through acceleration. This technique has been shown to lead to atomic mixing at the interface and consequently to a very strong adhesion of the film to the substrate. Moreover, the easily-controllable energy of the incoming ions via the substrate bias allows the formation of very smooth and dense thin films, usually less likely to fail under stress<sup>15</sup>.

Figure 4 shows the evolution of oxygen atomic fraction in the films and deposition rate as a function of oxygen residual pressure. This shows that a minimum pressure of  $5 \times 10^{-4}$  Torr has to be used in order to obtain a stoichiometric aluminum oxide. The film deposition rate decreases with increasing pressure, due to the reduction of the ion mean free path. Consequently, in order to maintain a reasonable deposition rate associated with the formation of a stoichiometric oxide, a residual pressure of  $5 \times 10^{-4}$  Torr has been chosen.

These experimental conditions were applied for the formation of  $\text{Al}_{2-x}\text{Er}_x\text{O}_3$  thin films. Two techniques were studied. The first approach was to use two separate filtered arc sources (one Al and one Er gun), as depicted in fig. 1. The two guns were pulsed alternately. This technique allows the control of the Er content over a wide range by setting the pulse length of the two sources in the required ratio, taking the different deposition rates of Al and

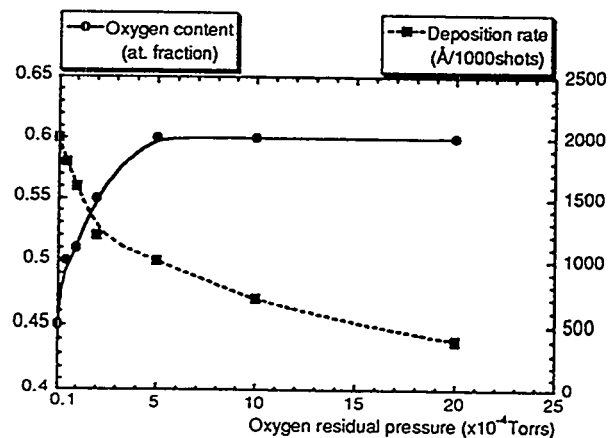


Figure 4 Evolution of oxygen atomic fraction and deposition rate as a function of oxygen residual pressure in  $\text{Al}_2\text{O}_3/\text{Si}$  thin films.

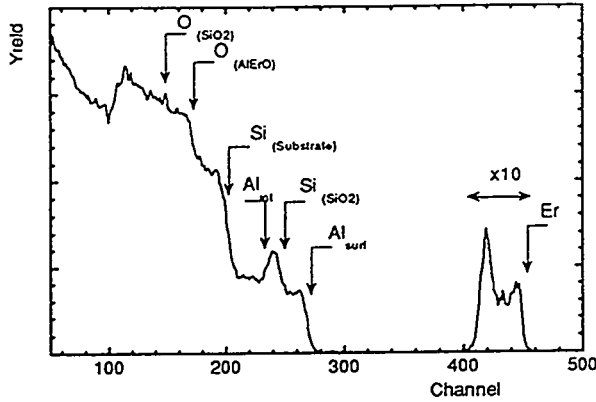


Figure 5 RBS spectrum of a  $\text{Al}_2\text{Er}_{0.05}\text{O}_3/\text{SiO}_2/\text{Si}$  structure (2000Å/2000Å/Si). Two guns technique.

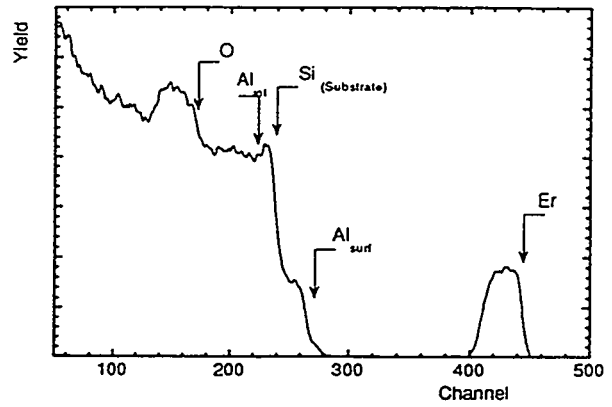


Figure 6 RBS spectrum of a  $\text{Al}_{1.92}\text{Er}_{0.08}\text{O}_3/\text{Si}$  structure (2000Å/Si). single gun with Al/Er(10%).

Er into account. Figure 5 shows the RBS spectrum of an  $\text{Al}_2\text{Er}_{0.005}\text{O}_3$  (2000Å) deposited on a  $\text{SiO}_2$  (2000Å)/Si substrate. As can be seen, this two gun technique is not ideal for very low concentration erbium doping of  $\text{Al}_2\text{O}_3$  thin films. Indeed, the concentration of erbium fluctuates throughout the depth of the sample. This problem is not encountered at higher doping concentrations and for a single gun technique as can be seen in figure 6. For this example, we have used a single gun fitted with an Er/Al alloy cathode and an erbium atomic fraction of 10%. We obtain a 2000Å thick film with a composition of  $\text{Al}_{1.92}\text{Er}_{0.08}\text{O}_3$  and an homogeneous erbium concentration as a function of depth in the film.

## OPTICAL PROPERTIES

As discussed in the introduction, the  $1.53\mu\text{m}$  emission of erbium ions is of great interest for optical telecommunications. This infrared emission originates from a  $4f^{11}$  incomplete shell transition between the  $^4I_{13/2}$  and the  $^4I_{15/2}$  level. This  $4f^{11}$  shell being well screened by outer closed orbitals  $5s^2$  and  $5p^6$ , the optical transitions of erbium are almost insensitive to the ion environment and to temperature. When these erbium ions are incorporated in a dielectric matrix, direct absorption can be used to excite the different transitions. For example, the 488nm and 514.5nm lines of an  $\text{Ar}^+$  ion laser correspond to the  $^4F_{7/2}$  and  $^2H_{11/2}$  absorption lines of erbium. The emission of a GaInAs laser diode can be adjusted to the absorption of the  $^4I_{11/2}$  level at  $\lambda=980\text{nm}$ . Once excited on an absorbing level, the population of the  $^4I_{13/2}$  level occurs via a complex multiphononic and/or photonic de-excitation. This well known energy transfer bring into play many Er-Er energy coupling effects which are of importance at high rare-earth concentration, such as cross relaxation, self-quenching phenomena or other upconversion processes<sup>21-22</sup>. The aluminum oxide erbium-doped samples are luminescent at room temperature as shown in figure 7 for a 3000Å-thick  $\text{Al}_{1.95}\text{Er}_{0.05}\text{O}_3$  thin film grown on silicon.

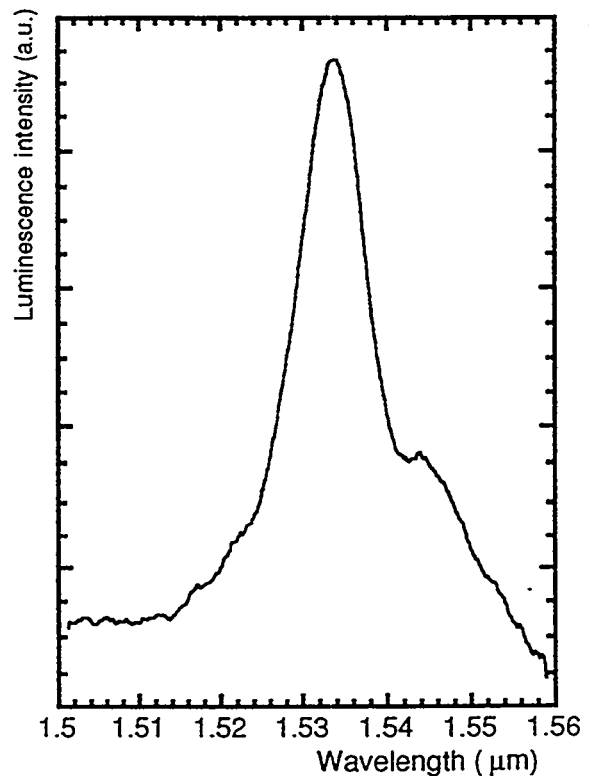


Figure 7 Room temperature photoluminescence spectrum under excitation at  $\lambda=488\text{nm}$  of a  $\text{Al}_{1.95}\text{Er}_{0.05}\text{O}_3/\text{Si}$  (3000Å) thin film.

## CONCLUSION

We have applied the MePIIID technology for the synthesis of  $\text{Al}_2\text{O}_3$  and  $\text{Al}_{2-x}\text{Er}_x\text{O}_3$  thin films. We have shown that this new tool can lead to very homogeneous thin films with a controllable erbium concentration and very smooth texture on a sub-micrometer scale. The erbium shows luminescence at  $1.53\mu\text{m}$  and at room temperature under excitation by an argon ion laser. The fabrication of multilayer structures such as  $\text{Al}_2\text{O}_3/\text{Al}_{2-x}\text{Er}_x\text{O}_3/\text{Al}_2\text{O}_3/\text{Si}$  is feasible, allowing the fabrication of optical integrated waveguides. Further studies are needed to determine the refractive index evolution of the material as a function of composition for calculation of the waveguide geometry and its performance compared to other synthesis techniques. However, this preliminary study indicates that high performance OEICs can be made, using a rapid, economic technology that can be scaled up to industrial parameters.

This Work was supported by the U.S. Department of Energy under contract No. DE-AC03-76SF00098.

## REFERENCES

1. Integrated optics: devices and applications. edited by J.T. Boyd. (IEEE, New York, NY, 1990)
2. S. R. Forest, Proc. IEEE, vol. 75, 11, 1488-97, (1987).
3. M. Federighi, I. Massarek, P. F. Trwoga, Electr. Lett., Vol. 30 No 11, 1277-82, (1994).
4. M. Oguma, T. Kitagawa, K. Hattori, M. Horiguchi. IEEE Phot. Tech. Lett., Vol 6, No 5, 1041 (1994).
5. O. Lumholt, T. Rasmussen, A. Bjarklev. Electr. Lett. Vol 29, No 5, 495, (1993).
6. K. Hattori, T. Kitagawa, M. Oguma, Y. Ohmori, M. Horigushi. Electr. Lett. Vol 30, No 11, 856 (1994)
7. G. N. Van den Hoven, E. Snoeks, A. Polman, J. W. M. van Uffelen, Y. S. Oei, M. K. Smit, Appl. Phys. Lett. 62, 24, 3065, (1993).
8. E. Lallier, J. P. Pocholle, M. Papuchon, Q. He, M. De Micheli, D. B. Ostrowsky, C. Grezes-Breset, E. Pelletier, Electr. Lett., Vol 28, No 15, 1428, (1992).
9. M. Lui, R. A. MacFarlane, D. Yap and D. Lederman, Electr. Lett. 29, 2, 172, (1993).
10. D. Marcuse, Theory of dielectric optical waveguides, Acad. Press, (1974)
11. R. M. Emmons, B. N. Kurdi, D. G. Hall, IEEE J. Quant. Elect. 28, 1, (1992).
12. A.S. Barrière, S. Raoux, A. Garcia, H. L'Haridon, D. Moutonnet and B. Lambert, J. Appl. Phys. 75, 2, 1133, (1994).
13. Rare Earth doped semiconductors. edited by G. S. Pomrenke, P. B. Klein and D. W. Langer. (Mater. Res. Soc. Proc., Vol. 301, 1993).
14. X. Godechot, M. B. Salmeron, D. F. Ogletree, J. E. Galvin, R. A. Galvin, R. A. MacGill, M. R. Dickinson, K. M. Yu and I. G. Brown, Mat. Res. Soc. Symp. Proc., Vol. 190, 95, (1991).
15. A. Anders, S. Anders, I. G. Brown, M. R. Dickinson and R. A. Macgill, J. Vac. Sci. Technol. B, 12, 2, 815, (1994).
16. S. Anders, A. Anders, M. Rubin, Z. Wang, S. Raoux, F. Kong and I. G. Brown, ICMCTF-95, San Diego, April 24-28, (1995).
17. I. G. Brown, M. R. Dickinson, J. E. Galvin, X. Godechot and R. A. MacGill, Nucl. Inst. Meth. Phys. Res. B, 55, 506, (1991).
18. I. I. Aksenov, V. A. Belous, V. G. Padalka, V. M. Khoroshikh, Sov. J. Plasma Phys. 4, 425, (1978).
19. A. Anders, S. Anders, and I. G. Brown, J. Appl. Phys. 75, 10, 4900, (1994).
20. S. Anders, A. Anders, and I. G. Brown, J. Appl. Phys. 75, 10, 4895, (1994)
21. F. Di Pasquale, M. Zoboli, M. Federighi, I. Massarek, IEEE J. Quant. El. 30, 5, 1277, (1994).
22. A. Lupei, V. Lupei, S. Georgescu, I. Ursu, V. I. Zhekov, T. M. Murina, A. M. Prokhorov, Phys. Rev. B. 41, 16, (1990).